COMPOSITE DESIGN AND MANUFACTURING

Composite Design and Manufacturing, 2025, **1(1)**, 58–68
https://doi.org/10.1093/cdm/wqaf005
Review Article

Review of finite element modelling of composite structures subjected to extreme loading conditions

Zhongwei Guan [1,*]

[1]Advanced Materials Research Centre, Technology Innovation Institute, P.O. Box 9639, Masdar City, Abu Dhabi, United Arab Emirates

*Corresponding author. Advanced Materials Research Centre, Technology Innovation Institute, P.O. Box 9639, Masdar City, Abu Dhabi, United Arab Emirates. E-mail: zhongwei.guan@tii.ae

Downloaded from academic.oup.com/cdm/article/1/1/wqaf005/8257362 by guest on 01 October 2026

Abstract

Although lightweight composites have been studied extensively, modelling their damage processes remains a challenging task. This is mainly due to the complexity of anisotropic failure mechanisms of fibre and matrix as well as interaction between the composite and other materials, especially under the load with high strain rate such as blast. This paper presents a brief review of numerical modelling of composite laminates and sandwich structures subjected to blast loading. In blast, structures undergo large plastic deformations or failure under a surged pressure within a very short time duration. The review covers different approaches to simplify impulsive loading, available constitutive relationships, failure criteria, and damage evolution laws in modelling of various constituent materials in composites. Although extensive work has been undertaken on modelling blast responses of various composite structures, capture of the perforation failure characteristics remains a challenging task. More advanced failure criteria and damage evolution mechanisms are required to tackle this problem. The review also presents modelling examples published.

Keywords: blast; finite element; composite laminates; sandwich structures; failure criteria

1. Introduction

With more uncertainties in the modern world due to possible terrorist threats or natural disasters, the blast response and resistance of composite structures become increasingly important issues to engineering communities and government bodies. In the initial stage of the explosion, an impulsive pressure, much greater than the static collapse pressure of the structures, is produced by shock wave in a very short time. This extremely high pressure forces the structures to undergo large plastic deformations and collapse or perforation failure, associated with energy absorption. In order to enhance energy absorption and blast resistant performance of composite structures, a deep insight into the explosion loading characteristics and the relationship between such load and the structural deformation/failure behaviour is required.

Testing the blast response of the composite structures is very time consuming, in addition to material and manpower costs. When conducting experimentally based research, tests should cover as many scenarios as possible, such as stacking configurations, constituent materials, geometries, loading and boundary conditions, etc. Therefore, the optimization process is likely to be very expensive and hugely time consuming. In contrast, the development of computer models using finite element (FE) analyse is a relatively quick and inexpensive process. In such circumstances, only a limited number of material tests and structural blast tests are required for validation purposes. Once computer models are validated against the corresponding blast test results, covering both the upper and lower bound cases, systematically designed parametric studies can be undertaken using validated numerical models.

In a bid to take advantage of their attractive dynamic properties and overall light weight, engineers have been investigating the energy-absorbing characteristics of sandwich structures when subjected to blast loading [1–10]. To date, much of this work has focused on the effect of underwater blast loading on the response of sandwich panels [1–7]. However, a number of workers have investigated the response of sandwich panels to conditions associated with air blast [8–10]. Jamil *et al.* [11] studied blast response of aluminium/thermoplastic polyurethane sandwich panels through experimental work and numerical analysis. Zheng *et al.* [12] undertook the experimental and numerical studies on the dynamic response of steel plates subjected to confined blast loading. The results from numerical simulations demonstrated that the maximum plastic deformation decreases greatly with increasing the mass ratio of the stiffener to the steel plate. It was also found that the stiffener location (on the side or opposite side of loading) has an insignificant influence on the deformation modes of the stiffened plates subjected to confined blast loading.

Modelling work using the commercial code ABAQUS/Explicit was undertaken on the blast responses of metal foam-based sandwich structures [13–16], metal honeycomb-based sandwich structures [17–19], as well as polyvinyl chloride (PVC) foam or balsa wood core-based sandwich structures [20–22]. LS-DYNA was also extensively used to model the blast behaviour of metal foam-based sandwich panels [23–25], skull sandwich structures [26], and sandwich panels [27]. 3D MOSAIC analysis approach was used to investigate the shock loading response of sandwich panels with 3D woven composite skins and a stitched foam core [28]. Guan *et al.* [29] and Hassan *et al.* [21] modelled blast response

Received: 5 May 2025; **Revised:** 8 June 2025; **Accepted:** 21 June 2025
© The Author(s) 2025. Published by Oxford University Press on behalf of Taiyuan University of Technology.
This is an Open Access article distributed under the terms of the Creative Commons Attribution License (https://creativecommons.org/licenses/by/4.0/), which permits unrestricted reuse, distribution, and reproduction in any medium, provided the original work is properly cited.

of foam-core sandwich structures. Langdon *et al.* [30] provided a comprehensive review on the response of polymeric composite structures subjected to air blast loading.

Blast behaviour of fibre metal laminates (FMLs) has also been studied extensively. Fleisher [31] investigated the blast resistance of an FML luggage container based on a design similar to that currently used by the civil air transport sector. The FML container comfortably contained a Lockerbie-type explosion, highlighting the enormous potential offered by these structures. Unfortunately, the increased cost associated with the manufacture of these structures has limited their more widespread use in this safety–critical environment. Recently, the blast resistance of FMLs based and on 2024 aluminium alloy and a glass fibre-reinforced polypropylene has been investigated [32–35]. In this study, tests have been conducted on FMLs based on 12 different stacking configurations, offering total laminate thicknesses up to 15 mm. In addition, Vo *et al.* [36, 37] and Sitnikova *et al.* [38, 39] modelled the blast response of FMLs. They developed modelling techniques to simulate the blast response of FMLs subjected to low-impulse and high-impulse blast loadings.

In recent years, 3D printed lattice structures were extensively studied to investigate their energy absorption capabilities and blast resistance. Al Mahria *et al.* [40] evaluated the dynamic response of triply periodic minimal surfaces (TPMSs) subjected to high strain rate compression. They found that diamond structure demonstrates the highest specific energy absorption (SEA) value of 35.57 J/g under the high strain rate loading condition, in comparison to 30.85 J/g in the quasi-static loading. The study suggests that TPMS structures could be potential candidates not only for quasi-static, but also for dynamic applications related to a high strain rate loading. Santiago *et al.* [41] modelled and optimized TPMS-based lattices subjected to high strain rate impact loadings. Ramos *et al.* [42] carried out experimental evaluation of hybrid lattice structures subjected to blast loading. The results have demonstrated that TPMS topology and relative density changes substantially affect its performance.

Although reasonably extensive work has been undertaken on modelling blast responses of various composite structures, capture of the perforation failure characteristics remains a challenging task. More advanced failure criteria and damage evolution mechanisms are required to tackle this problem. This review focuses on numerically described blast loading with acceptable simplifications, constitutive models, failure criteria, and damage evolution laws used to simulate the blast response of the composite structures mentioned below. These cover FMLs, carbon and glass fibre-reinforced laminates. The sandwich structures reviewed include PVC foam core-based ones with composite skins or metal skins, metallic foam core with metallic skins and metallic cellular core with metallic skins, together with the author's work in this field.

2. Characterizing and modelling blast loads

To model the blast behaviour of composite laminates and sandwich structures, the mechanisms of blast pressure building up after detonation need to be modelled in the first instance. Blast is an extreme dynamic loading process. In the process of an explosion, the blast travels as an incident wave until it strikes an object. Upon striking the object, a reflected wave is generated which travels back towards the point of explosion. At a point, some distance from the centre of the explosion, the reflected wave meets the incident wave, producing a single vertical wave front. The structure below the point of intersection of the reflected wave and the incident wave experiences a single shock, whereas the surface above this point experiences a shock history, which is a resultant of the incident and reflected wave. During the blast processes, the pressure builds up to a peak value of an excessive pressure. The pressure then decays to a local ambient pressure in a time point to a partial vacuum of very small amplitude and eventually returns to the ambient pressure. The portion of the pressure–time history below zero is referred to as the "negative or suction phase" and the portion above zero is called the "positive phase", which has a little effect on the response of structures [43]. A typical pressure–time history for a blast wave was given by Kinney and Graham [44].

In most blast studies, the negative phase of the blast wave is ignored, and only the parameters associated with the positive phase are considered since it is generally accepted that the damage to the structure is caused by the positive phase [13, 14]. The positive impulse of the wave during the positive phase can be give as

$$I = \int_{t_a}^{t_a + t_d} P(t)dt \tag{1}$$

where $P(t)$ is the positive pressure as a function of time, t_a and t_d are the arrival time and the duration of positive phase, respectively.

There are different forms of $P(t)$ proposed by researchers, which is often described by exponential functions such as the Friedlander equation [45, 46]

$$P(t) = P_{SO}[1 - \frac{t}{t_d}] \exp\left\{-\frac{bt}{t_d}\right\} \tag{2}$$

In the above equation, b is the decay factor which is a function of the peak pressure P_{SO}. The pressure-time profile is shown in Fig. 1.

The simplified profile was also used by researchers [15, 17, 47, 48]. A triangular blast and Heaviside pulse was also proposed [49] and used [50], i.e.

$$P(t) = P_{SO}[1 - \frac{t}{t_d}][H(t) - \delta_b H(t - t^* t_d)] \tag{3}$$

In the above equation, $H(t)$ denotes the Heaviside step function, δ_b is a tracer that can be taken as 1 or 0 depending on whether the sonic-boom or triangular blast load is considered, t^* denotes the shock pulse length factor. Based on Friedlander equation in Equation (2), a modified Friedlander equation can be obtained.



Figure 1. Schematic diagram of a pressure–time pulse.

Downloaded from academic.oup.com/cdm/article/1/1/wqaf005/8257362 by guest on 01 October 2026

In numerical modelling of blast load, apart from the pressure–time profile, pressure–location relation also needs to be considered. For a square laminated plate subjected to surface explosion, the pressure function $P(r, t)$ was proposed [51] and the pressure pulse shape was implemented with AUTODYN [33].

$$P(r,t) = p_1(r)p_2(t) \tag{4}$$

where

$$p_1(r) = \begin{cases} P_{SO} & r \le r_0 \\ P_{SO}e^{-k(r-r_0)} & r_0 < r < r_b \\ 0 & r > r_b \end{cases}$$

$$p_2(t) = e^{-2t/t_d}$$

In Equation (5), r_0 is the radius of the explosive disc used in the experiments [33], k is an exponential decay constant, which models the pressure distribution over the exposed area of the plate, $r_b < L/2$, L being the length of the panel. The decay constant $k(I)$ with the variation of the total impulse, I, used in the numerical simulations can be interpolated. The total impulse is defined as

$$I = 2\pi \int_0^{\infty} \int_0^{r_b} P(r,t) r dr dt \tag{6}$$

Vo *et al.* [35] implemented both Equations (4) and (5) into ABAQUS/Explicit through a user-defined subroutine. The less computational expensive ConWep algorithm [52] used to describe air blast loading is also available in LS-DYNA and ABAQUS/Explicit. Other simplified or idealized pressure–time profiles were proposed [53, 54].

3. Modelling of composite laminates and sandwich structures

Composite structures subjected to blast loading can be modelled based on modelling blast response of their constituent materials and bonding between them. Such structures are made of monolithic materials or cellular solids. There are several constitutive relationships, failure criteria, and damage evolution mechanisms available to determine their corresponding dynamic behaviour under blast loading conditions. In addition, several contact algorithms are also available to model interaction between constituent materials.

3.1 Modelling metallic materials

There are three commonly used material models for metals subjected to high strain rate loading. The Johnson–Cook constitutive model is perhaps the most widely used one at present, which can be used to describe metal plasticity under large strain, high strain rate, and temperature conditions [55, 56].

$$\bar{\sigma} = [A + B(\bar{\varepsilon}_{pl})^n][1 + C\ln\left(\frac{\dot{\bar{\varepsilon}}_{pl}}{\dot{\varepsilon}_o}\right)][1 - \left(\frac{T - T_{room}}{T_{melt} - T_{room}}\right)^m] \tag{7}$$

where $\bar{\sigma}$ is the equivalent stress, $\bar{\varepsilon}_{pl}$ is the equivalent plastic strain, n is a strain hardening index, $\dot{\bar{\varepsilon}}_{pl}$ is the equivalent plastic strain rate, $\dot{\varepsilon}_o$ is the reference strain rate, T_{melt} and T_{room} are the melting and transitive temperatures, respectively and A, B, C, and m are material constants.

The Johnson–Cook damage law [56] can be used to simulate failure of the metals. This model is given as

$$\varepsilon_f = [D_1 + D_2 \exp\left(D_3 \frac{p}{\bar{\sigma}}\right)][1 + D_4 \ln\left(\frac{\dot{\bar{\varepsilon}}_{pl}}{\dot{\varepsilon}_o}\right)][1 + D_5\left(\frac{T - T_{room}}{T_{melt} - T_{room}}\right)] \tag{8}$$

where ε_f is the equivalent strain to fracture at the current conditions of strain rate, temperature, pressure, and equivalent stress, p is a pressure stress, D_1–D_5 are damage parameters.

For rate-dependent metallic materials, the uniaxial flow rate is expressed as the following relationship:

$$\dot{\bar{\varepsilon}}_{pl} = h(\bar{\sigma}, \bar{\varepsilon}_{pl}, T) \tag{9}$$

where h is a known function. The rate-dependent hardening curves in terms of the static relation can be expressed as [57]

$$\bar{\sigma}(\bar{\varepsilon}_{pl}, \dot{\bar{\varepsilon}}_{pl}) = \sigma_y(\bar{\varepsilon}_{pl}) R(\dot{\bar{\varepsilon}}_{pl}) \tag{10}$$

where R is a stress ratio. Both shear failure and tensile failure were used to simulate the failure mechanisms of aluminium alloys [35].

Another constitutive relationship, namely the Cowper–Symonds relation, can be employed, if only the strain rate effect is considered. In this relation, strain rate is calculated for time duration from the start to the point when the strain is nearly constant from the equivalent plastic strain–time history [58], i.e.

$$\sigma_{dy} = \bar{\sigma}\left(1 + \left|\frac{\dot{\bar{\varepsilon}}_{pl}}{D}\right|^{1/n}\right) \tag{11}$$

where σ_{dy} is the dynamic yield stress, D and n are material constants.

3.2 Modelling fibre-reinforced materials

Fibre-reinforced composite laminates are often modelled as an anisotropic linear elastic material prior to the onset of damage, followed by damage evolution controlled either by fracture energy or element-based failure displacement. A damage mechanics approach may be suitable to predict composite damage in high strain rate loading conditions, such as blast. Kachanov [59] and Rabotnov [60] originally developed the damage mechanics approach, which was initially applied to composites by Frantziskonis [61]. It can be used to accurately determine the full range of deterioration in a composite material, from no damage to full damage with material disintegrated. Neto *et al.* [62] and Krajcinovic [63] gave a detailed review of issues in the area of damage mechanics and a historical overview. This approach has been used to predict different composite failure modes, such as matrix cracks, fibre fracture and delamination, and even compression behaviour. Hashin's failure criteria [64, 65] are the popular ones for modelling onset damage of fibre-reinforced composites, which are implemented in a 2D form in commercial codes such as ABAQUS and LS-DYNA. These criteria employ four damage initiation mechanisms, i.e. fibre tension, fibre compression, matrix tension, and matrix compression. Other mode-dependent failure criteria were also developed by researchers [66–68].

In order to take material response through its thickness into account, Vo *et al.* [35] implemented Hashin's 3D failure criteria into ABAQUS/Explicit through a user-defined subroutine, which are

Tensile fibre mode: $\sigma_{11} > 0$

$$\text{If } \left(\frac{\sigma_{11}}{X_{1t}}\right)^2 + \left(\frac{\sigma_{12}}{S_{12}}\right)^2 + \left(\frac{\sigma_{13}}{S_{13}}\right)^2 = 1,\ d_{ft} = 1 \tag{12}$$

Compressive fibre mode: $\sigma_{11} < 0$

Downloaded from academic.oup.com/cdm/article/1/1/wqaf005/8257362 by guest on 01 October 2026

$$\text{If } \frac{|\sigma_{11}|}{X_{1c}} = 1,\ d_{fc} = 1 \tag{13}$$

Tensile matrix mode: $\sigma_{22} + \sigma_{33} > 0$

$$\text{If } \frac{(\sigma_{22}+\sigma_{33})^2}{X_{2t}^2} + \frac{\sigma_{23}^2 - \sigma_{22}\sigma_{33}}{S_{23}^2} + \frac{\sigma_{12}^2+\sigma_{13}^2}{S_{12}^2} = 1,\ d_{mt} = 1 \tag{14}$$

Compressive matrix mode: $\sigma_{22} + \sigma_{33} < 0$

$$\text{If } [\left(\frac{X_{2c}}{2S_{23}}\right)^2 - 1]\frac{(\sigma_{22}+\sigma_{33})}{X_{2c}} + \frac{(\sigma_{22}+\sigma_{33})^2}{4S_{23}^2} + \frac{(\sigma_{23}^2 - \sigma_{22}\sigma_{33})}{S_{23}^2} + \frac{\sigma_{12}^2+\sigma_{13}^2}{S_{12}^2} = 1,\ d_{mc} = 1 \tag{15}$$

In these failure criteria, damage variables d_{ft} and d_{fc} associate with fibre tension and compression failure modes, respectively; and d_{mt} and d_{mc} associate with the corresponding failure modes in the matrix. Besides, lamina strength allowable values for tension and compression in the lamina principle material directions (fibre or 1—direction and matrix or 2—direction) as well as the in-plane shear strength allowable value are denoted by X_{1t}, X_{1c}, X_{2t}, X_{2c}, and S_{12}, respectively, and S_{13} and S_{23} are allowable values for the transverse shear strength. The degradation of stiffness matrix (**C**) [69] components due to fibre and matrix failure can be expressed as

$$\begin{aligned} C_{11} &= (1-d_f)C_{11}^0 \\ C_{ij} &= (1-d_f)(1-d_m)C_{ij}^0,\ \ i,j = 1,2,3 \\ C_{ii} &= (1-d_f)(1-s_{mt}d_{mt})(1-s_{mc}d_{mc})C_{ii}^0,\ \ i = 4,5,6 \end{aligned} \tag{16}$$

where global fibre and matrix damage variables are also defined as

$$\begin{aligned} d_f &= 1-(1-d_{ft})(1-d_{fc}) \\ d_m &= 1-(1-d_{mt})(1-d_{mc}) \end{aligned} \tag{17}$$

They are either taken as 0 (no damage) and 1 (complete damage) in the code. The factors s_{mt} and s_{mc} in the definitions of the shear moduli are introduced to control the loss of shear stiffness caused by tensile and compressive failure of the matrix, respectively.

Iannucci [70] implemented a damage model into the explicit dynamic FE code LLNL DYNA3D [71] to predict a woven composite on a layer-by-layer basis (2D), with damage parameters as

Fibre fracture in the local warp fibre bundles for each ply, d_1
Fibre fracture in the local weft fibre bundles for each ply, d_2
Fibre matrix deterioration due to in-plane shear for each ply, d_3

The damage variables are in the range from 0 to 1, with the former representing an undamaged material and the latter a complete failure. The damage terms in the stiffness degradation matrix are as follows:

$$\frac{1}{Z}\begin{bmatrix} (1-d_1)E_{11}^0 & (1-d_2)(1-d_1)\nu_{12}^0 E_{22}^0 & 0 \\ (1-d_2)(1-d_1)\nu_{21}^0 E_{11}^0 & (1-d_1)E_{11}^0 & 0 \\ 0 & 0 & ZG_{12}^0(1-d_1) \end{bmatrix} \tag{18}$$

where

$$Z = 1-(1-d_1)(1-d_2)\nu_{12}^0\nu_{21}^0 > 0$$

The superscript zero represents material properties in the virgin state.

The simplest damage evolution is modelled by the negative slope of the equivalent stress–displacement relation after damage initiation is achieved, as shown in Fig. 2. Fracture energies for fibre tension, fibre compression, matrix tension, and matrix compression failure modes need to be specified to indicate energies dissipated during damage. Nahas [72] carried out progressive failure analysis based on the failure predictions of a modified maximum strain criterion. The degradation function defined in Equation (19) is displayed in Fig. 3.

$$\sigma = \sigma_{\max} e^{(-a(\varepsilon-\varepsilon_{\max})/n\varepsilon_{\max})} \tag{19}$$

Here, a and n are empirical constants. Iannucci [70] proposed a 2D damage evolution law for all damage modes in the local coordinate system, which is given by

$$\dot{d}_i = \alpha_i\left(\left(\frac{\bar{\sigma}_{jk}}{S_{jk}}\right)^2 - 1\right) \tag{20}$$

where d_i is the damage parameters for mode i (i=1, 2, 3), α_i and S_{jk} (j, k =11, 22, 12) are material constants in this simple form. For initiation of nucleation, effective stress $\bar{\sigma}_{jk}$ needs to be greater than the in-plane lamina strength S_{jk}. A similar form to Equation (20) was also proposed by Nemes and Spéciel [73]. A thorough review on degradation models for progressive failure analysis of fibre-reinforced polymer composites is given by Garnich and Akula [74].

3.3 Modelling cellular solids

Metal foams, PVC foams, and honeycombs are cellular solids, which can absorb considerable energy through plastic dissipation in compression. Their cellular microstructures make them undergo large deformations at nearly constant nominal stress [75, 76]. As a result, they are usually used as core materials for sandwich structures in order to absorb impact and blast shock energy. Constitutive relations are given in terms of the effective stress [77] as

$$\bar{\sigma} = Y^0 + Q_1(1-e^{-c_1 r}) + Q_2(1-e^{-c_2 r}) \tag{21}$$

where Y^0 is the uniaxial yield stress, r_1 and r_2 are the damage plastic strain accumulated, the rest are the hardening parameters. Based on a self-similar yield surface model, Deshpande and Fleck [78] developed a constitutive model to describe metal foam undergoing continuous crushing, which is given by

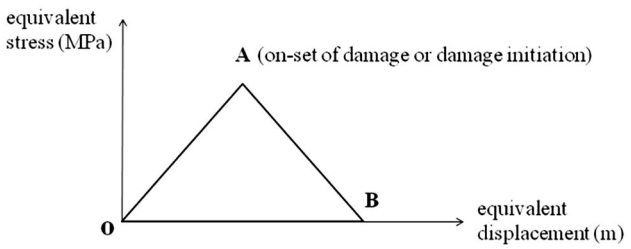


Figure 2. Energy dissipation due to damage.

Downloaded from academic.oup.com/cdm/article/1/1/wqaf005/8257362 by guest on 01 October 2026

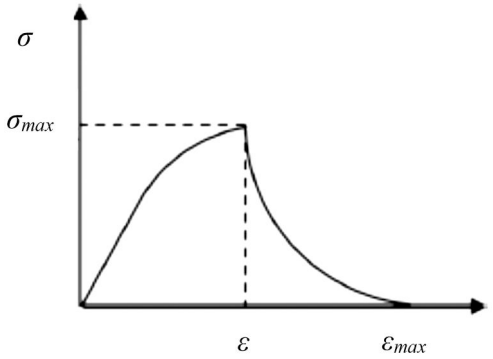


Figure 3. Nahas unloading model.

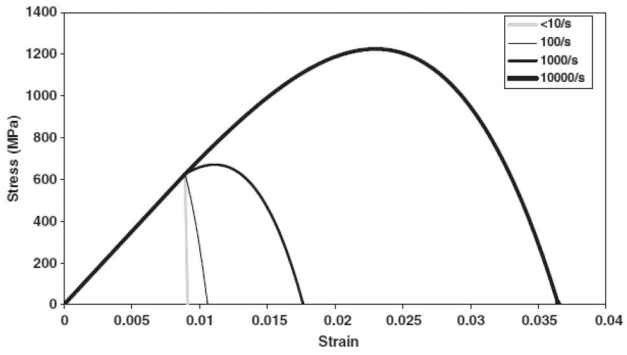


Figure 4. Strain rate dependence for tensile loadings [38].

$$\sigma_y^2 \equiv \frac{1}{\left[1+\left(\frac{\alpha}{3}\right)^2\right]}\left[\bar{\sigma}^2+\alpha^2\sigma_m^2\right] \tag{22}$$

Here, α defines the shape of the yield surface, σ_m is the mean stress, and σ_y is the yield strength of the foam in uniaxial tension or compression. This constitutive model was also used to model truss core [13] and aluminium honeycomb core [23] and PVC foam core [21, 22] subjected to blast loading.

3.4 Rate dependence

Fibre-reinforced composites are essentially rate-dependent materials when they are subjected to high strain rates, such as under blast loading [79, 80]. General conclusions indicate that an increase in strain rate induces an increase in tensile failure stress and strain; however, the initial modulus appears to be unaffected. Figure 4 shows the strain rate response with material constants set as $\alpha_i = 1000/s$ and $S_{jk} = 610\,\text{MPa}$ (Equation (20)). The curves are generated via a single element subject to varying strain rates.

Based on the work by Yen and Caiazzo [81], Yen [82], and Daniel *et al.* [83], Vo *et al.* [35] considered strain rate effects on material properties and strengths as follows:

$$\{E_{RT}\} = \{E_0\}\left(1 + C_1 ln\frac{\dot{\bar{\varepsilon}}}{\dot{\varepsilon}_0}\right) \tag{23}$$

$$\{S_{RT}\} = \{S_0\}\left(1 + C_2 ln\frac{\dot{\bar{\varepsilon}}}{\dot{\varepsilon}_0}\right) \tag{24}$$

Here, C_1 and C_2 are the strain rate constants, $\dot{\varepsilon}_0$ is the reference strain rate, $\{E_0\}$ are the elastic moduli of $\{E_{RT}\}$ at the reference strain rate and $\{S_0\}$ are the strength values of $\{S_{RT}\}$ at the reference strain rate.

Different commercial FE codes have different special functions, advantages, and disadvantages. Table 1 shows a few software packages commonly used for modelling fibre-reinforced composite laminates and sandwich structures.

4. Some modelling work undertaken

Extensive numerical modelling has been undertaken on structural responses of composite laminates and sandwich structures subjected to blast. The work is mainly carried out by using commercial codes with built-in constitutive models, failure criteria, and damage evolution or by developing in-house programmes. Karagiozova *et al.* [36] using the ABAQUS/Explicit code simulated the response of FMLs subjected to low impulsive localized blast loading. Blast responses of GLARE fuselage [84] and panels [85] were also simulated using LS-DYNA. A non-linear transient analysis of FMLs under blast loads was carried out using the mixed finite element method (FEM) by Aksoylar *et al.* [86]. Vo *et al.* [36, 37] developed a vectorized user material subroutine (VUMAT) and implemented it in ABAQUS/Explicit to model blast behaviour of woven glass–fibre in a polypropylene (GFPP) composite inside FMLs, with strain rate effects considered. Sitnikova *et al.* [38] developed an instant failure model to simulate perforation failure of GFPP layers inside FMLs subjected to high implusive blast loading. A number of dynamic failure scenarios were captured, such as petalling, large tensile tearing, and multiple debonding between the aluminium and GFPP layers. Figure 5 shows a typical comparison of the predicted displacement contour plots with the experimental data. A comprehensive review on the FE analysis of blast response of FMLs using FE codes (ABAQUS, LS-DYNA, etc.) was also given by Serubibi *et al.* [87]. Patton and Hart [88] undertook experimental and computational investigation on the damage mechanisms of composite metal hybrid panels under blast loading. FE models were developed by using LS-DYNA to simulate the blast apparatus and hybrid composite panel. Using ABAQUS/Explicit, Zhu *et al.* [89] carried out the numerical investigation on effects of blast loading on anti-fragment performance of hollow cylindrical UHMWPE cross-ply laminate. They implemented a strain rate-dependent, orthotropic, elastoplastic constitutive model with progressive failure through a user subroutine (VUMAT) in the commercial code ABAQUS/Explicit to model UHMWPE laminates.

Modelling work using commercial code ABAQUS/Explicit was undertaken on blast responses of metal foam-based sandwich structures [13–16], metal honeycomb-based sandwich structures [17–19], as well as PVC foam-based sandwich structures [21, 22]. Figure 6 shows some simulated and experimental failure modes of PVC foam-based sandwich panels with aluminium alloy skins. LS-DYNA was also used to model blast behaviour of metal foam-based sandwich panels [23, 24], skull sandwich structures [26], and composite laminates [90, 91]. 3D MOSAIC analysis approach was used to investigate shock loading response of sandwich panels with 3D woven composite skins and stitched foam core [27]. Alanbay and Batra [92] carried out research on optimization of sandwich structures with fibre-reinforced skins and PVC foam core to mitigate blast loading. The deformations of the sandwich structure and the shock pressure generated by detonating a charge were modelled using the commercial FE code ABAQUS. Liang *et al.* [93] investigated the synergistic effect of combined blast loads on UHMWPE fibre mesh-reinforced polyurea composites. They used ANSYS software to conduct the frequency analysis to obtain the first three modal characteristics, such as the natural frequencies and mode shapes. The dynamic response of

Downloaded from academic.oup.com/cdm/article/1/1/wqaf005/8257362 by guest on 01 October 2026

Table 1. Summary of common commercial codes and their features in modelling blast response of fibre-reinforced composite laminates and sandwich structures

Commercial code	Constitutive model	Failure criteria	Applicability	Limitation and difficulty
ANASYS	• Orthotropic elasticity • 2D/3D Hashin • Puck (inter-fibre failure) • Continuum damage mechanics (CDM) • Nonlinear shear behaviour	• Hashin (fibre/matrix failure) • Tsai–Wu • Puck (for compression) • Cohesive zone model (CZM)	• Suitable for unidirectional prepreg (ACP) and woven fabric	• ANSYS itself does not directly offer the 3D Hashin criteria • Limit on handling high strain rate modelling ($<10^2$ s^{-1}) • Puck model less refined than in ABAQUS • Delamination modelling requires manual set-up
LS-DYNA	• MAT_54/55 (composite damage) • MAT_58 (Laminated composite fabric) • MAT_261 (progressive damage) • MAT_262 (orthotropic with failure)	• 2D and 3D Hashin criteria • Tsai–Wu failure criterion • Chang–Chang (fibre/matrix failure) • Strain-based failure	• Suitable for unidirectional prepreg and woven fabric • Accurate modelling of blast loading • Validation against experimental data available in the code. • Fluid modelling • Robust element deletion for damage	• Need user-defined subroutine to handle extreme strain rate • Requires expertise in keyword editing • Limited built-in delamination models
ABAQUS/Explicit	• Orthotropic elasticity • Continuum damage mechanics (CDM) • Volumetric hardening foam (sandwich core) • Johnson–Cook (metal layer in FMLs)	• 2D Hashin criteria • Puck (matrix compression) • Cohesive zone model (CZM) • Crushable foam (Deshpande and Fleck) • Johnson–Cook damage model	• Suitable for unidirectional prepreg (2D Hashin) and woven fabric (CDM) • Python scripting for automation	• CONWEB underestimates blast loading • Converging issue related to high strain rate loading • Challenge to gain rate-dependent material properties • Need user-defined subroutine to deal with extreme strain rate
AUTODYN	• Orthotropic elastic–plastic • Johnson–Holmquist (for brittle composites) • SPH for fibre breakage	• Principal stress/strain failure • Johnson–Cook (for metal matrix composites) • Erosion criteria (element deletion)	• Optimized for blast/impact • SPH and Euler methods for fibre breakage • Efficient for explicit events	• Limited static/delamination analysis • Fewer composite-specific models • Less user-friendly for lay-up definition



Figure 5. Comparison of the predicted displacement contour plots with the experimental data [37].

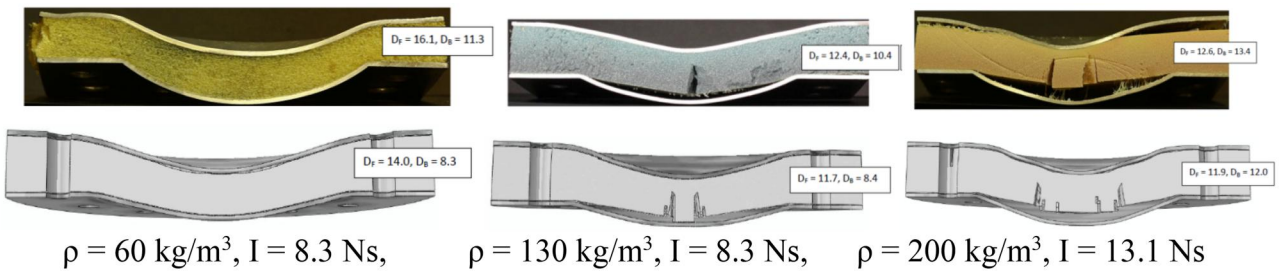


Figure 6. Comparisons of failure modes obtained from tests (top) and FE simulations (bottom) [21].

Downloaded from academic.oup.com/cdm/article/1/1/wqaf005/8257362 by guest on 01 October 2026

composite tube-reinforced porous polyurethane structures subjected to far field underwater blast loading was studied by Liu *et al.* [94]. Using the first-order Mooney–Rivilin fitting parameters, a quasi-static compression numerical simulation model was established with C3D8R elements by ABAQUS software. Eulerian elements were applied to model water, and Lagrangian elements are used to establish other components in the FE modelling using ABAQUS/Explicit.

Some researchers developed in-house numerical programmes to simulate responses of various composite structures under explosive loads. Librescu *et al.* [49, 95] studied dynamic behaviour of sandwich panels and active aeroelastic control of aircraft composite wings to blast loading, with governing equation systems in the von Kármán sense. Sandwich plates/panels subjected to blast loadings were also modelled numerically by the basic equations of the dynamic theory of advanced curved panels [96] and laminated composite rectangular plates [97]. In addition, in-house FE codes were developed to model blast response of fibre-reinforced composites [46, 47, 98] and sandwich plates [7, 99–101] to underwater explosive loads and air blast loads.

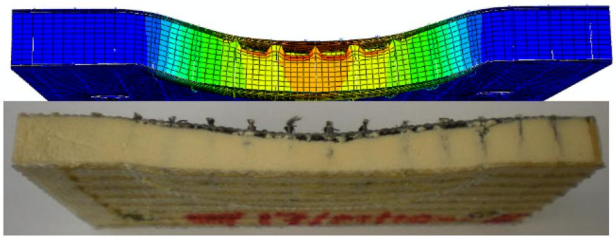


Figure 7. Comparison of the experimental and numerical failure modes for a stitched sandwich panel subjected to an impulse of 5.47 Ns.

Figure 7 shows the comparison of failed central cross-sections of the panel subjected to 5.47 Ns impulse obtained from the experiment and the numerical modelling [28]. Some basic features are well simulated, such as significant thinner in the central part of the panel and debonding between the top skin and the core.

A stitched sandwich panel subjected to a high impulse of 11.08 Ns is shown in Fig. 8. The complete failure of the back face along the support boundary is well simulated, i.e. there is a punch through disc. The simulated PVC foam core also indicates a shear failure on the boundary of impulsive pressure on the front face. Moreover, local damages where stitches are through can be clearly seen.

Figure 9 shows the simulation results of TPU-core aluminium skin sandwich panels subjected to blast loading [11]. The deformation profiles indicate a very good correlation for the core of the TPU with AA 2024-T3 skins. The separation of the TPU core and AA 2024-T3 skins are consistent in all cases, where some rebound of the TPU was observed for the simulations, as was the case with the experiments.

Recently, modelling blast response of syntactic foam structures made of aluminium matrix and ceramic hollow microspheres was studied [25]. The simulations were performed for the syntactic foams with two different thicknesses in order to predict different damage patterns observed during experiments.

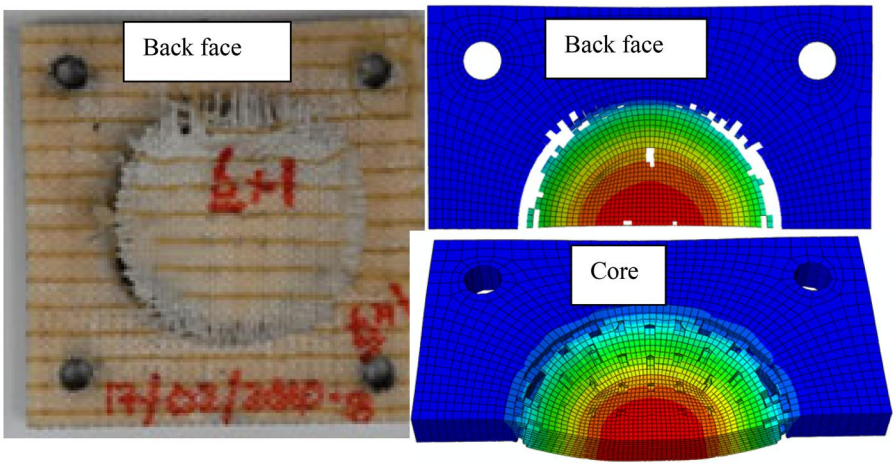


Figure 8. Experimental and simulated back face of a stitched sandwich panel subjected to an impulse of 11.08 Ns [29].

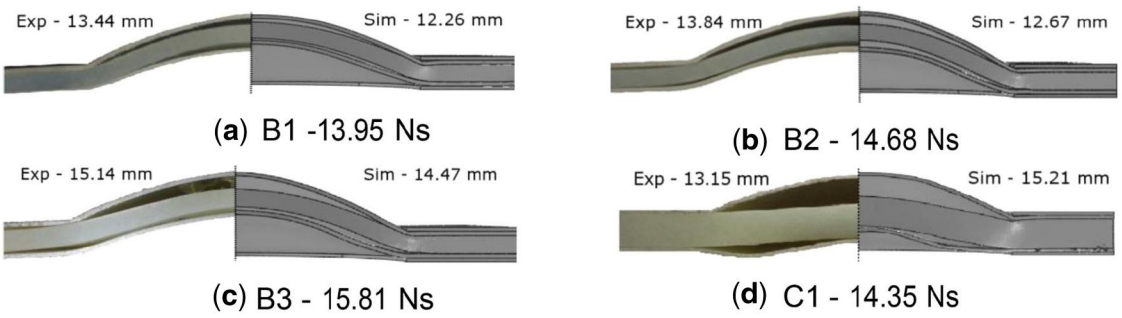


Figure 9. Comparison of the experimental and modelled displacement profiles of TPU-core sandwich panels at the central cross-sections [11]. (a) B1—13.95 Ns. (b) B2—14.68 Ns. (c) B3—15.81 Ns. (d) C1—14.35 Ns.

Downloaded from academic.oup.com/cdm/article/1/1/wqaf005/8257362 by guest on 01 October 2026

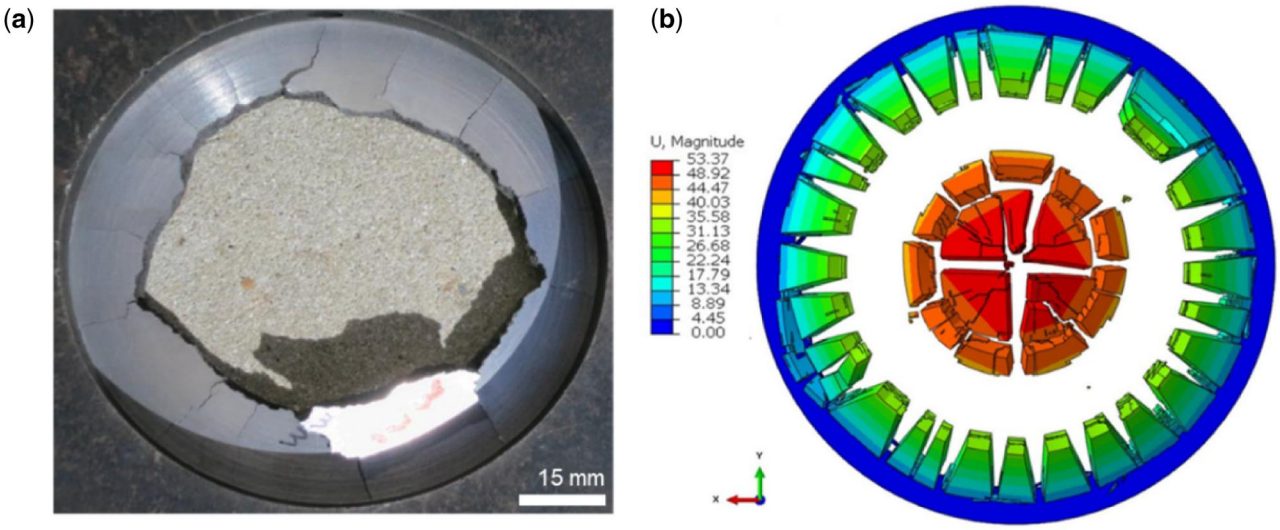


Figure 10. Failure mode of a 3 mm thick syntactic foam subjected to a blast impulse of 2 Ns: (a) experimental and (b) FEA [25].

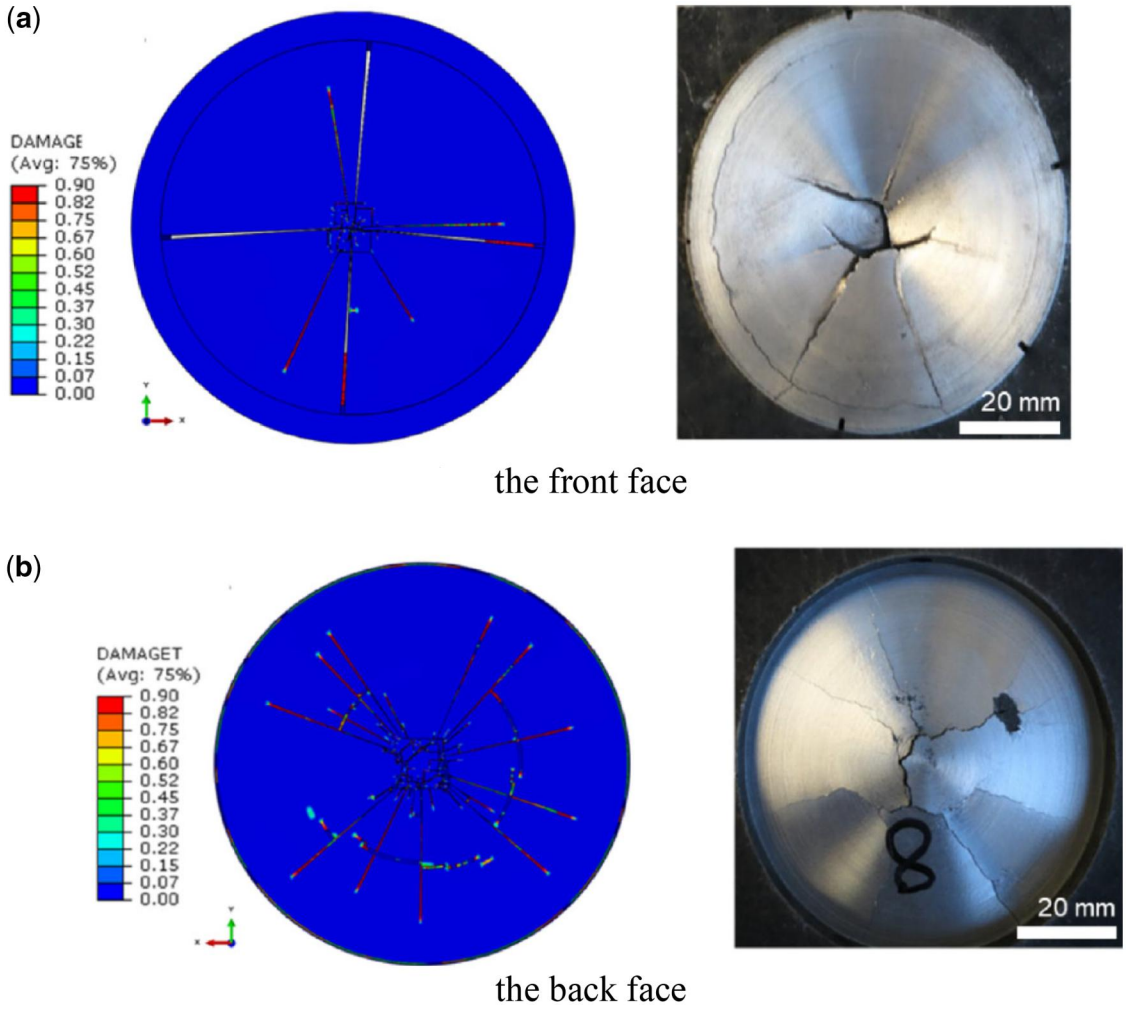


Figure 11. Comparison of the predicted and experimental damage profiles of the 14 mm thick syntactic foam subjected to an impulse of 4.82 Ns [25]. (a) The front face and (b) the back face.

Downloaded from academic.oup.com/cdm/article/1/1/wqaf005/8257362 by guest on 01 October 2026

Figure 10 shows the validation on the damage profiles on the front and back face of the foam panels of a thin sample (thickness = 3 mm) subjected to an impulse of 2 Ns.

The blast response of a thick foam panel (thickness = 14 mm) subjected to an impulse of 4.82 Ns is also modelled for validation of the model to capture the related damage profile without the total failure. Figure 11 shows the simulated failure mode in comparison to the experimental one with reasonable correlation.

5. Summary

Numerical modelling work of fibre-reinforced composite laminates and various sandwich structures subjected to blast loadings has been reviewed. Before carrying out modelling of structural response, explosive loading has to be simplified to reflect the most important characteristics. Several approaches commonly adopted, either in chart or equation forms, are discussed. A majority of the estimations on the effective duration of blast loading is 10 s of microseconds (usually less than 40 μs); however, some are assumed in minisecond (ms). As there is no precise measurement of such duration, even taking it as 10 or 20 or 30 μs, there will be a big difference on calculations of the impulsive pressure. This affects numerical modelling greatly. Therefore, in order to simulate blast response accurately, the reasonable estimation of the blast duration is crucial.

Modelling of metallic constituent materials is relatively simple, since commonly used constitutive models and failure criteria are available in commercial FE codes. Johnson–Cook rate-dependent plasticity with damage (degradation) measures is a good model, which is capable of capturing various failure modes of metals. However, accurate material parameters, covering rate-dependent plastic hardening, temperature-dependent behaviour as well as damage constants, are essential. In addition, modelling of cellular structures, such as metal foams, truss cores, honeycombs, and polymer foams, seems well addressed. The crushable foam model has been approved by a large number of researchers as an effective approach to simulate the corresponding blast response.

In comparison, modelling blast behaviour of fibre-reinforced composites still remains a challenging task, especially involving simulation of perforation failure. Most of the published work deals with the blast response in relation to relatively low impulsive pressures, which do not cause perforation failure of fibre-reinforced composites. Yet mainly only 2D failure criteria and damage evolution are available in commercial FE codes, which do not take the structural response through the thickness into account. The possible reason is that the failure mechanisms of fibre debonding and breaking under an extremely high strain rate are not well captured in the existing programmes. It seems fine to simulate the response up to the onset of failure, also delamination between layers by cohesive elements. Therefore, it is necessary to develop and implement 3D failure criteria and damage evolution laws with appropriate description of high strain rate dependence to simulate progressive failure of fibres with numerical stability (convergent rate).

Acknowledgements

The author would like to acknowledge the use of the UK National e-Infrastructure Service in carrying out this work.

Conflict of interest

None declared.

Funding

The author would like to thank the Leverhulme Trust (UK) for providing partial financial support (F/00025/AO) for this research.

References

[1] Makinen K. The transverse response of sandwich panels to an underwater shock wave. *J Fluids Struct* 1999;**13**:631–46.
[2] Liang Y, Spuskanyuk AV, Flores SE *et al.* The response of metallic sandwich panels to water blast. *J Appl Mech* 2007;**74**:81–99.
[3] Tilbrook MT, Deshpande VS, Fleck NA. Underwater blast loading of sandwich beams: regimes of behaviour. *Int J Solids Struct* 2009; **46**:3209–21.
[4] Spuskanyuk AV, McMeeking M. Sandwich panels for blast protection in water: simulations. *Int J Mat Res* 2007;**98**:1250–5.
[5] Perotti LE. Modeling the behavior of fiber reinforced sandwich structures subjected to underwater explosions. Ph.D. Thesis, California Institute of Technology, 2010.
[6] Mori LF, Queheillalt DT, Wadley HNG *et al.* Deformation and failure modes of I-core sandwich structures subjected to underwater impulsive loads. *Exp Mech* 2009;**49**:257–75.
[7] Andrews EW, Moussa NA. Failure mode maps for composite sandwich panels subjected to air blast loading. *Int J Impact Eng* 2009;**36**:418–25.
[8] Hoo Fatt MS, Palla L. Analytical modeling of composite sandwich panels under blast loads. *J Sandwich Struct Mater* 2009; **11**:357–80.
[9] Hutchinson JW, Xue Z. Metal sandwich plates optimised for pressure pulses. *Int J Mech Sci* 2005;**47**:545–69.
[10] Nurick GN, Langdon GS, Chi Y *et al.* Behaviour of sandwich panels subjected to intense air blast—part 1: experiments. *Compos Struct* 2009;**91**:433–41.
[11] Jamil A, Guan ZW, Cantwell WJ *et al.* Blast response of aluminium/thermoplastic polyurethane sandwich panels—experimental work and numerical analysis. *Int J Impact Eng* 2019; **127**:31–40.
[12] Zheng C, Kong XS, Wu WG *et al.* Experimental and numerical studies on the dynamic response of steel plates subjected to confined blast loading. *Int J Impact Eng* 2018;**113**:144–60.
[13] Xue Z, Hutchinson JW. Preliminary assessment of sandwich plates subject to blast. *Int J Mech Sci* 2003;**45**:687–705.
[14] Qiu X, Deshpande VS, Fleck NA. Finite element analysis of the dynamic response of clamped sandwich beams subject to shock loading. *Eur J Mech A/Solid* 2003;**22**:801–14.
[15] Qiu X, Deshpande VS, Fleck NA. Dynamic response of a clamped circular sandwich plate subject to shock loading. *J Appl Mech* 2004;**71**:637–45.
[16] Radford DD, Mcshane GJ, Deshpande VS *et al.* The response of clamped sandwich plates with metallic foam cores to simulated blast loading. *Int J Solids Struct* 2006;**43**:2243–59.
[17] Mori LF, Lee S, Xue ZY *et al.* Deformation and fracture modes of sandwich structures subjected to underwater impulsive loads. *J Mech Mater Struct* 2007;**2**:1981–2006.
[18] Wei Z, He MY, Evans AG. Application of a dynamic constitutive law to multilayer metallic sandwich panels subject to impulsive loads. *J Appl Mech* 2007;**74**:636–44.
[19] Theobald MD, Nurick GN. Experimental and numerical analysis of tube-core claddings under blast loads. *Int J Impact Eng* 2010;**37**:333–48.
[20] Tagarielli VL, Deshpande VS, Fleck NA. Prediction of the dynamic response of composite sandwich beams under shock loading. *Int J Impact Eng* 2010;**37**:854–64.

Downloaded from academic.oup.com/cdm/article/1/1/wqaf005/8257362 by guest on 01 October 2026

[21] Hassan MZ, Guan ZW, Cantwell WJ *et al.* The influence of core density on the blast resistance of foam-based sandwich structures. *Int J Impact Eng* 2012;**50**:9–16.
[22] Langdon GS, Karagiozova D, von Klemperer CJ *et al.* The air-blast response of sandwich panels with composite face sheets and polymer foam cores: experiments and predictions. *Int J Impact Eng* 2013;**54**:64–82.
[23] Zhu F, Zhao L, Lu G *et al.* A numerical simulation of the blast impact of square metallic sandwich panels. *Int J Impact Eng* 2009;**36**:687–99.
[24] Jing L, Wang Z, Zhao L. Dynamic response of cylindrical sandwich shells with metallic foam cores under blast loading—numerical simulations. *Compos Struct* 2013;**99**:213–23.
[25] Al Teneiji M, Krishnan K, Guan ZW *et al.* Dynamic response of aluminium matrix syntactic foams subjected to high strain-rate loadings. *Compos Struct* 2023;**303**:116289.
[26] Gu L, Chafi MS, Ganpule S *et al.* The influence of heterogeneous meninges on the brain mechanics under primary blast loading. *Compos B Eng* 2012;**43**:3160–6.
[27] Hong S, McConnell J. Influences of material properties on energy absorption of composite sandwich panels under blast loading. *J Compos Constr* 2012;**16**:464–76.
[28] Tekalur SA, Bogdanovich AE, Shukla A. Shock loading response of sandwich panels with 3-D woven E-glass composite skins and stitched foam core. *Compos Sci Tech* 2009;**69**:736–53.
[29] Guan ZW, Aktas A, Potluri P *et al.* The blast resistance of stitched sandwich panels. *Int J Impact Eng* 2014;**65**:137–45.
[30] Langdon GS, Cantwell WJ, Guan ZW *et al.* The response of polymeric composite structures to air-blast loading: a state-of-the-art. *Int Mater Rev* 2014;**59**:159–77.
[31] Fleisher HJ. Design and explosive testing of a blast resistant luggage container. In: *Proceedings of the Structures Under Shock and Impact Conference IV*. Ashurst, Southampton, UK: WIT Press, 1996, 51–9.
[32] Lemanski SL, Langdon GS, Nurick GN *et al.* Behaviour of fibre-metal laminates subjected to localised blast loading: part I—experimental observations. *Int J Impact Eng* 2007;**34**:1202–22.
[33] Langdon GS, Nurick GN, Lemanski SL *et al.* Failure characterisation of blast-loaded fibre-metal laminate panels based on aluminium and glass-fibre reinforced polypropylene. *Compos Sci Technol* 2007;**67**:1385–405.
[34] Langdon GS, Nurick GN, Lemanski SL *et al.* Behaviour of fibre-metal laminates subjected to localised blast loading: part II—quantitative analysis. *Int J Impact Eng* 2007;**34**:1223–45.
[35] Karagiozova D, Langdon GS, Nurick GN *et al.* Simulation of the response of fibre-metal laminates to localised blast loading. *Int J Impact Eng* 2010;**37**:766–82.
[36] Vo TP, Guan ZW, Cantwell WJ *et al.* Low-impulse blast behaviour of fibre-metal laminates. *Compos Struct* 2012;**94**:954–65.
[37] Vo TP, Guan ZW, Cantwell WJ *et al.* Modelling of the low-impulse blast behaviour of fibre–metal laminates based on different aluminium alloys. *Compos B Eng* 2013;**44**:141–51.
[38] Sitnikova E, Guan ZW, Cantwell WJ *et al.* Modelling of perforation failure in fibre metal laminates subjected to high impulsive blast loading. *Int J Solids Struct* 2014;**51**:3135–46.
[39] Sitnikova E, Guan ZW, Cantwell WJ. The analysis of the ultimate blast failure modes in fibre metal laminates. *Compos Sci Technol* 2016;**135**:1–12.
[40] Al Mahria S, Santiago R, Lee D-W *et al.* Evaluation of the dynamic response of triply periodic minimal surfaces subjected to high strain-rate compression. *Addit Manuf* 2021;**8**:102220.
[41] Santiago R, Ramos H, AlMahri S *et al.* Modelling and optimisation of TPMS-based lattices subjected to high strain-rate impact loadings. *Int J Impact Eng* 2023;**177**:104592.
[42] Ramos H, Pickering E, AlMahri S *et al.* Experimental evaluation of hybrid lattice structures subjected to blast loading. *Add Manuf* 2023;**76**:103751.
[43] Brode HL. *Numerical Solution of Spherical Blast Waves*. New York: American Institute of Physics, 1955.
[44] Kinney GF, Graham KJ. *Explosive Shocks in Air*, 2nd edn. New York: Springer-Verlag, 1985.
[45] Kinney GF. *Explosive Shocks in Air*. New York: The Macmillan Company, 1962.
[46] Hetherington J, Smith P. *Blast and Ballistic Loading of Structures*. London: CRC Press, 1994, 396.
[47] Batra RC, Hassan NM. Response of fiber reinforced composites to underwater explosive loads. *Compos B Eng* 2007;**38**:448–68.
[48] Batra RC, Hassan NM. Blast resistance of unidirectional fiber reinforced composites. *Compos B Eng* 2008;**39**:513–36.
[49] Marzocca P, Librescu L, Chiocchia G. Aeroelastic response of 2D lifting surfaces to gust and arbitrary explosive loading signature. *Int J Impact Eng* 2001;**25**:67–85.
[50] Librescu L, Oh S-Y, Hohe J. Linear and non-linear dynamic response of sandwich panels to blast loading. *Compos B Eng* 2004;**35**:673–83.
[51] Bonorchis D, Nurick GN. The influence of boundary conditions on the loading of rectangular plates subjected to localised blast loading—importance in numerical simulations. *Int J Impact Eng* 2009;**36**:40–52.
[52] Hyde D. *ConWep, Conventional Weapons Effects Program*. Vicksburg, MS: US Army Engineer Waterways Experiment Station, 1992.
[53] Rajamani A, Prabhakaran R. Response of composite plates to blast loading. *Exp Mech* 1980;**20**:245–50.
[54] Thiagarajan G, Hsia KJ, Walters W. Blast simulation of armor plate behavior using the virtual internal bond model. In: *16th ASCE Engineering Mechanics Conference, 16–18 July*. Seattle: University of Washington, 2003.
[55] Johnson GR, Cook WH. 1983. A constitutive model and data for metals subjected to large strains, high strain rates and high temperatures. In: *Proceedings of the 7th International Symposium on Ballistics*, the Hague, the Netherlands.
[56] Johnson GR, Cook WH. Fracture characteristics of three metals subjected to various strains, strain rates, temperatures and pressures. *Eng Fract Mech* 1985;**21**:31–48.
[57] Stout MG, Pollansbee PS. Strain rate sensitivity, strain hardening, and yield behaviour of 304L stainless steel. *J Eng Mater Technol* 1986;**108**:344–53.
[58] Cowper GR, Symonds PS. Strain hardening and strain rate effect in the impact loading of cantilever beams. Report No. 28, Brown University, 1957.
[59] Kachanov LM. Time of rupture process under creep conditions. *Izy Akad Nank SSR Otd Tech Nauk* 1958;**8**:26–31.
[60] Rabotnov YN. Creep rupture. In: *Proceedings of the XII International Congress Applied Mechanics*. Springer: Stanford, 1968.
[61] Frantziskonis S. Distributed damage in composites, theory and verification. *Compos Struct* 1988;**10**:165–84.
[62] Neto E, Peric D, Owen, DRJ. Continuum modelling and numerical simulation of material damage at finite strains. *Arch Comput Methods Eng* 1998;**5**:311–84.
[63] Krajcinovic D. Damage mechanics: accomplishments, trends and needs. *Int J Solids Struct* 2000;**37**:267–77.
[64] Hashin Z, Rotem A. A fatigue criterion for fiber-reinforced materials. *J Compos Mater* 1973;**7**:448–64.

Downloaded from academic.oup.com/cdm/article/1/1/wqaf005/8257362 by guest on 01 October 2026

[65] Hashin Z. Failure criteria for unidirectional fiber composites. *J Appl Mech* 1980;**47**:329–34.
[66] Lee JD. Three-dimensional finite element analysis of damage accumulation in composite laminates. In: Proceedings of the Second USA–USSR Symposium, *9–12 March*. Bethlehem, PA: Martinus Nijhoff Publisher, 1982, 291–306.
[67] Christensen RM. Stress based yield/failure criteria for fiber composites. *Int J Solids Struct* 1997;**34**:529–43.
[68] Mayes JS, Hansen AC. A multicontinuum failure analysis of composite structural laminates. *Mech Adv Mater Struct* 2001; **8**:249–62.
[69] Tong L, Mouritz AP, Bannister MK. *3D Fibre Reinforced Polymer Composites*. Amsterdam, Holland: Elsevier, 2002.
[70] Iannucci L. Progressive failure modelling of woven carbon composite under impact. *Int J Impact Eng* 2006;**32**:1013–43.
[71] Hallquist JO, Whirley RG. DYNA3D user manual, nonlinear dynamic analysis in three dimensions. Report UCID-19592, Rev. 5, University of California, 1989.
[72] Nahas MN. Yield and ultimate strengths of fibre composite laminates. *Compos Struct* 1986;**6**:283–94.
[73] Nemes JA, Spéciel E. Use of a rate-dependent continuum damage model to describe strain-softening in laminated composites. *Comput Struct* 1996;**58**:1083–92.
[74] Garnich MR, Akula VMK. Review of degradation models for progressive failure analysis of fiber reinforced polymer composites. *Appl Mech Rev* 2009;**62**:010801-1–010801-33.
[75] Gibson LJ, Ashby MF. *Cellular Solids: Structure and Properties*, 2nd edn. Cambridge: Cambridge University Press, 1997.
[76] Hanssen AG, Enstock L, Langseth M. Close-range blast loading of aluminium foam panels. *Int J Impact Eng* 2002;**27**:593–618.
[77] Lemaitre J. *A Course on Damage Mechanics*, 2nd edn. Berlin: Springer, 1996.
[78] Deshpande VS, Fleck NA. Multi-axial yield behaviour of polymer foams. *J Mech Phys Solids* 2000;**48**:1859–66.
[79] Harding J. Impact damage in composite materials. *Sci Eng Compos Mater* 1989;**1**:41–68.
[80] Li Z, Lambros J. Dynamic thermomechanical behaviour of fiber reinforced composites. *Compos A* 2000;**31**:537–47.
[81] Yen CF, Caiazzo A. Innovative processing of multifunctional composite armor for ground vehicles. Arl-CR-484, US Army Research Laboratory, Aberdeen Proving Ground, MD, 2001.
[82] Yen CF. Ballistic impact modeling of composite materials. In: Proceedings of the 7th International LS-DYNA Users Conference. Detroit: Ansys Inc, 2002, 15–23.
[83] Daniel IM, Werner BT, Fenner JS. Strain-rate-dependent failure criteria for composites. *Compos Sci Technol* 2011;**71**:357–64.
[84] Kotzakolios T, Vlachos DE, Kostopoulos V. Blast response of metal composite laminate fuselage structures using finite element modelling. *Compos Struct* 2011;**93**:665–81.
[85] Soutis C, Mohamed G, Hodzic A. Modelling the structural response of GLARE panels to blast load. *Compos Struct* 2011; **94**:267–76.
[86] Aksoylar C, Ömercikoğlu A, Mecitoğlu Z *et al.* Nonlinear transient analysis of FGM and FML plates under blast loads by experimental and mixed FE methods. *Compos Struct* 2012; **94**:731–44.
[87] Serubibi A, Hazell PJ, Escobedo JP *et al.* Fibre-metal laminate structures: high-velocity impact, penetration, and blast loading—a review. *Compos A* 2023;**173**:107674.
[88] Patton EG, Hart RJ. Experimental and computational investigation into the damage mechanisms in composite metal hybrid panels subjected to high pressure blast loading. *Int J Impact Eng* 2024;**190**:104970.
[89] Zhu W, Yao W, Huang G *et al.* Numerical investigation on effects of blast loading on anti-fragment performance of hollow cylindrical UHMWPE cross-ply laminate. *Compos Struct* 2025;**351**:118565.
[90] Wei Z, Shetty MS, Dharani LR. Stress characteristics of a laminated architectural glazing subjected to blast loading. *Comput Struct* 2006;**84**:699–707.
[91] LeBlanc J, Shukla A. Dynamic response of curved composite panels to underwater explosive loading: experimental and computational comparisons. *Compos Struct* 2011;**93**:3072–81.
[92] Alanbay B, Batra RC. Optimization of blast mitigating sandwich structures with fiber-reinforced face sheets and PVC foam layers as core. *Thin-Walled Struct* 2022;**179**:109721.
[93] Liang M, Zhou M, Li X *et al.* Synergistic effect of combined blast loads on UHMWPE fiber mesh reinforced polyurea composites. *Int J Impact Eng* 2024;**183**:104804.
[94] Liu YZ, Li S, Lin X *et al.* Dynamic response of composite tube reinforced porous polyurethane structures under underwater blast loading. *Int J Impact Eng* 2023;**173**:104483.
[95] Librescu L, Na S, Qin Z *et al.* Active aeroelastic control of aircraft composite wings impacted by explosive blasts. *J Sound Vib* 2008;**318**:74–92.
[96] Hause T, Librescu L. Dynamic response of doubly-curved anisotropic sandwich panels impacted by blast loadings. *Int J Solids Struct* 2007;**44**:6678–700.
[97] Kazanci Z. Dynamic response of composite sandwich plates subjected to time-dependent pressure pulses. *Int J Non-Linear Mech* 2011;**46**:807–17.
[98] Mehar K, Panda SK, Dewangan HC. Multiscale finite element prediction of thermomechanical flexural strength of nanotube-reinforced hybrid smart composite panel bonded with SMA fibre. *Structures* 2020;**28**:2300–10.
[99] Nayak AK, Shenoi RA, Moy, SS, J. Transient response of initially stressed composite sandwich plates. *Finite Elem Anal Des* 2006; **42**:821–36.
[100] Tuzgel F, Akbulut EF, Guzel E *et al.* Testing and modeling blast loading of a sandwich structure cored with a bio-inspired (balanus) core. *Thin-Walled Struct* 2022;**175**:109185.
[101] Abdoh DA. Three-dimensional peridynamic modeling of damage and penetration in composite plates exposed to localized explosive blasts. *Comput Math Appl* 2024;**175**:399–415.

Downloaded from academic.oup.com/cdm/article/1/1/wqaf005/8257362 by guest on 01 October 2026

© The Author(s) 2025. Published by Oxford University Press on behalf of Taiyuan University of Technology.

This is an Open Access article distributed under the terms of the Creative Commons Attribution License (https://creativecommons.org/licenses/by/4.0/), which permits unrestricted reuse, distribution, and reproduction in any medium, provided the original work is properly cited.
Composite Design and Manufacturing, 2025, 1, 58–68
https://doi.org/10.1093/cdm/wqaf005
Review Article